Behavior of l-bits near the many-body localization transition

Abishek K. Kulshreshtha,[1] Arijeet Pal,[1,2] Thorsten B. Wahl,[1] and Steven H. Simon[1]
[1]*Rudolf Peierls Centre for Theoretical Physics, Clarendon Laboratory, Parks Road, Oxford OX1 3PU, United Kingdom*
[2]*Department of Physics and Astronomy, University College London, Gower Street, London WC1E 6BT, United Kingdom*

(Received 20 July 2017; revised manuscript received 31 August 2018; published 5 November 2018)

Eigenstates of fully many-body localized (FMBL) systems are described by quasilocal operators τ_i^z (l-bits), which are conserved exactly under Hamiltonian time evolution. The algebra of the operators τ_i^z and τ_i^x associated with l-bits ($\boldsymbol{\tau}_i$) completely defines the eigenstates and the matrix elements of local operators between eigenstates at all energies. We develop a nonperturbative construction of the full set of l-bit algebras in the many-body localized phase for the canonical model of MBL. Our algorithm to construct the Pauli algebra of l-bits combines exact diagonalization and a tensor network algorithm developed for efficient diagonalization of large FMBL Hamiltonians. The distribution of localization lengths of the l-bits is evaluated in the MBL phase and used to characterize the MBL-to-thermal transition.

DOI: 10.1103/PhysRevB.98.184201

I. INTRODUCTION

Dynamics of thermalization in closed, interacting quantum systems is a phenomenon of fundamental importance which has received considerable attention in the past decade [1]. Although states of matter at thermal equilibrium are widespread, the phenomenon of MBL has provided a novel paradigm for the breakdown of thermalization in quantum systems [2–6]. MBL has now been realized in several experiments using cold atoms and trapped ions and shown to be a robust phase [7,8]. MBL as a quantum phase of matter raises several exciting possibilities for realizing topological order in excited states and preserving quantum information [9–11]. Although MBL has been firmly established in one dimension [12,13], several questions related to its instability to thermalization at weaker disorder [14–16] and existence in higher dimensions remain hotly debated [17–19].

Many-body eigenstates of thermal systems are exponentially complex. On the other hand, for MBL in one-dimensional models with bounded local Hilbert spaces [20], an efficient description emerges when the entire spectrum is localized, due to an extensive set of local conservation laws given by the operators τ_i^z, known as *l-bits* [21–23]. Approximate τ_i^z operators represent the entire spectrum with exponential accuracy in terms of the quantum numbers of these operators, which scale only linearly with the size of the system. Such a structure of the eigenstates also implies the existence of quasilocal operators τ_i^x which produce transitions between two particular many-body eigenstates. For a spin-1/2 system, the τ_i^z and τ_i^x operators satisfy the Pauli spin algebra where the full many-body Hamiltonian is diagonal in the τ_i^z basis, and τ_i^x operators characterize the matrix elements between the eigenstates at all energies. Therefore, l-bits are analogous of bare spins, yet describe an interacting system over a range of parameters.

For finite-size MBL systems the l-bits can be constructed approximately using local unitary transformations [24–26]. The l-bits constructed in this perturbative manner only commute approximately with the Hamiltonian. The methods accessing the exact τ_i^z operators by studying the infinite time limit are not able to construct the algebra of the l-bit operators [27]. In this article we develop a nonperturbative construction of the set of τ_i^z and τ_i^x operators representing the l-bits in the MBL phase using a combination of tensor network methods [28–31] and exact diagonalization. In contrast to prior work, the l-bit algebras that we construct are exact and exponentially localized [24–26], i.e., the commutator of the set l-bit operators τ_i^z with the Hamiltonian is strictly zero. Our construction of l-bits allows us to study the behavior of the conserved quantities over a range of disorder strengths, even in the vicinity of the MBL-to-thermal transition.

By performing a finite-size scaling collapse of the l-bit localization length, the critical disorder strength and the correlation length exponent are extracted. For finite-size systems, the divergence of the localization length is cut off by the system size. The finite-size scaling function also provides an estimate of the crossover scale between the thermal and the quantum critical regimes. We characterize the distribution of localization lengths of the l-bits as a function of disorder. In the localized phase, the distribution has exponential tails which shows that the l-bits with large localization lengths are rare. On approaching the transition into the thermal phase, the distribution becomes heavy tailed with significant weight at localization lengths comparable to the system size. The heavy tails can be fitted to a power law. Due to finite-size effects, an exponential fit is also feasible. Thus, the l-bits with large localization lengths are no longer rare and can be destabilized by local perturbations which produce long-range resonances [12,13].

II. MODEL AND l-BIT PHENOMENOLOGY

We work with the one-dimensional XXZ spin chain in a random magnetic field, with the Hamiltonian

$$H = \sum_{i=1}^{L-1} \mathbf{S}_i \cdot \mathbf{S}_{i+1} + \sum_{i=1}^{L} h_i S_i^z, \tag{1}$$

where $\mathbf{S}_i = \frac{1}{2}\boldsymbol{\sigma}_i$ and each h_i is drawn randomly from a uniform distribution $[-h, h]$. The phase diagram of this model is well studied using exact diagonalization and has a phase transition from the thermal into the FMBL phase at $h_c \approx 3.5$ [4,32].

The set of Pauli operators $\{\boldsymbol{\sigma}_i\}$ define the physical bits ("p-bit" operators) which act on a local two-dimensional Hilbert space. At disorder strengths much larger than h_c, due to MBL of the full spectrum, the p-bits can be unitarily transformed into localized bits ("l-bit" operators). Each l-bit operator $\boldsymbol{\tau}_i$ is derived from the corresponding p-bit on site i, and has weights which decay exponentially with the distance from site i. The hallmark of the l-bits is the *exact* commutativity of all τ_i^z with the Hamiltonian for a finite-size system. These operators are constructed according to $\tau_i^z = U\sigma_i^z U^\dagger$, where U is an operator that diagonalizes the Hamiltonian and preserves the local structure. Matrices which diagonalize the Hamiltonian are nonunique. For example, the columns of any matrix diagonalizing the Hamiltonian can be permuted to form another matrix which also diagonalizes the Hamiltonian, yet these permutations affect the the locality of the τ_i^z operators. Therefore, not simply any choice of matrix U diagonalizing the Hamiltonian will successfully construct the most local set of τ_i^z.

III. CONSTRUCTION OF EXACT l-BIT ALGEBRAS

Due to the emergent integrability in the MBL phase, each eigenstate can be labeled by the set of eigenvalues $l_i = \pm 1$ of $\{\tau_i^z\}$. An eigenstate $|\alpha\rangle$ comes with its corresponding ordered string of $\{l_i^\alpha\}$, of length n that are either $+1$ or -1. We define the j partner of an eigenstate to be the eigenstate obtained by flipping the jth l-bit. We assign the j partner of $|\alpha\rangle$ as $|\beta_{j,\alpha}\rangle$ and they are said to be *paired* on site j. The structure of the partnering of eigenstates may not be unique and provides a representation of the l-bit operators, which are constructed from the eigenstates as given in Eqs. (2)–(4):

$$\tau_i^x = \sum_\alpha |\alpha\rangle\langle\beta_{i,\alpha}|, \tag{2}$$

$$\tau_i^y = -i\sum_\alpha l_i^\alpha |\alpha\rangle\langle\beta_{i,\alpha}|, \tag{3}$$

$$\tau_i^z = \sum_\alpha l_i^\alpha |\alpha\rangle\langle\alpha|. \tag{4}$$

In this construction, τ_i^x plays the role of a bit flip operator, similar to the σ_i^x Pauli matrix. For example, τ_2^x will flip the eigenstate $\{++\cdots\}$ to $\{+-+\cdots\}$. The network of allowed partner eigenstates are tightly constrained by the algebraic structure of the τ_i^x operators.

The action of the l-bit operators τ_i^z and τ_i^x on the eigenstates is simple. When τ_i^z acts on an eigenstate $|\alpha\rangle$, the eigenstate is returned with a sign ± 1 to match l_i^α. There are no off-diagonal matrix elements in the eigenstate basis. When τ_i^x acts on an eigenstate, it produces a transition to an eigenstate with the l-bit eigenvalue on site i being flipped. In this sense, the l-bits can be thought of as "dressed" p-bits and are related to them by a sequence of local unitary transformations, with weight exponentially decaying with distance from the l-bit's localization center.

In order to construct l-bit operators as described in Eqs. (2)–(4), we must find an eigenstate pairing structure (or a configuration of j partners) that creates quasilocal operators. The tensor network approach developed in [28] provides an efficient method to approximate the unitary U which transforms the Hamiltonian into a predominantly diagonal basis for an MBL system. The tensor network approximation encodes an l-bit structure for all approximate eigenstates. By matching exact eigenstates to these approximate ones, we can find a pairing scheme that produces quasilocal operators that exactly commute with the Hamiltonian. We begin by describing the tensor network algorithm and go on to describe the process of matching exact eigenstates to the approximate tensor network ones.

The tensor network approach described in Ref. [28] provides an efficient approximation of all eigenstates of MBL systems. This method employs a two-layer ansatz comprising local unitary rotations to transform trivial spin states to approximate MBL eigenstates. When stitched together, these layers of local unitary rotations create a unitary matrix that approximately diagonalizes the Hamiltonian of the system. This algorithm produces operators with limited support on the lattice; an l-bit operator produced by these methods has nontrivial support on a finite region and acts trivially everywhere else. However, it produces rotations that preserve local structure, so it determines an l-bit algebra over approximate eigenstates which can be used to construct exact l-bit operators.

Our goal is to craft $|\alpha\rangle$, $|\beta_{i,\alpha}\rangle$ pairings using the approximations given by the tensor network approach. The tensor network approximation yields a unitary matrix whose columns are approximate eigenstates $|a\rangle$ of the Hamiltonian. However, this unitary matrix does not exactly diagonalize the Hamiltonian. The columns of this unitary matrix encode a pairing structure on the approximate eigenstates, which we label $|a\rangle$, $|b_{i,a}\rangle$. This built-in pairing structure is given by the l-bit indices $\{l_i\}$ determined by the indexing of the unitary matrix. To impose this pairing structure on the exact eigenstates of a system, we attempt to find a one-to-one mapping that matches approximate eigenstates to exact eigenstates. A proper mapping will produce l-bit operators with quasilocal action and exact commutation with the Hamiltonian.

The purpose of this mapping procedure, which we call *matching*, is to assign each exact eigenstate a place in the l-bit spin structure. If an exact eigenstate $|\alpha\rangle$ is matched to an approximate eigenstate $|a\rangle$, with l-bit assignment $\{+-++-+\}$ for example, then the exact eigenstate is assigned the same l-bit label.

Matching approximate and exact eigenstates entails two parts: first finding approximate eigenstates and exact eigenstates with an inner product close to 1, and second matching the remaining eigenstates using an algorithm described below and in Fig. 1. Oftentimes, especially deep in the localized phase, many pairings are obvious as overlap between approximate eigenstates and exact eigenstates is high. In these cases, one can simply carry out the first part of the matching algorithm by finding the best matched approximate eigenstate for each exact eigenstate using the inner product and pairing them together. Closer to the phase transition, matchings are less obvious, requiring the use of the second part of the algorithm.

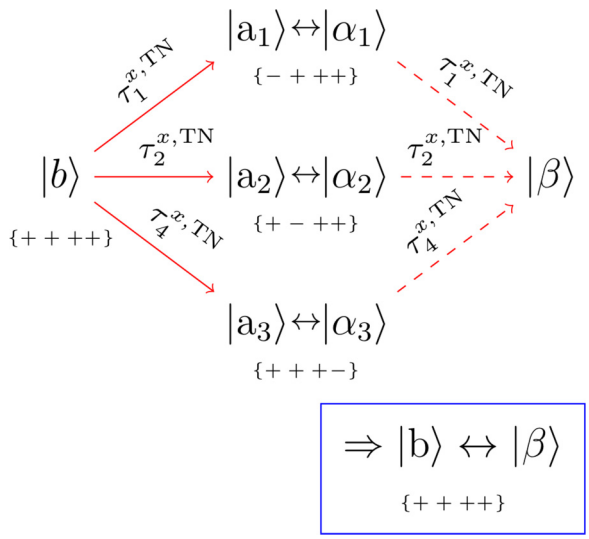

FIG. 1. Figure depicting a matching algorithm between tensor network approximate states and exact eigenstates. The set of approximate eigenstates has an existing pseudospin structure. Given a set of already matched approximate and exact states $|a_i\rangle$ and $|\alpha_i\rangle$, respectively, an approximate eigenstate $|b\rangle$ can be matched to an exact eigenstate $|\beta\rangle$ if the same transformation that exactly takes $|b\rangle$ to $|a_i\rangle$ (solid arrows) roughly takes $|\alpha_i\rangle$ to $|\beta\rangle$ (dashed arrows). This procedure takes advantage of the fact that $\tau_i^{x\,2} = 1$.

For the first part of the matching process, we match any eigenstates for which $|\langle\alpha||a\rangle| > t$, where t is some threshold. For our calculations, we set $t = 0.6$. Increasing the threshold increases computational cost, while decreasing it runs the risk of making poor assignments. When a match above the threshold is found, we match $|a\rangle$ to $|\alpha\rangle$ and assign $|\alpha\rangle$ the same l-bit label as $|a\rangle$, meaning that $l_i^a = l_i^\alpha$ and the set $\{|b_{i,a}\rangle\}$ corresponds to the set $\{|\beta_{i,\alpha}\rangle\}$. As expected, the number of matches above the threshold increases with increasing disorder. In systems with disorder $W = 3$ and below, a majority of matches may be below the threshold.

Because some eigenstates cannot be matched above this threshold, we utilize the second part of the matching process, using the already-matched states to inform the new matches. Consider $\{|\lambda_k\rangle\}$ the set of exact eigenstates matched to a tensor network approximate eigenstate $\{|l_k\rangle\}$ ($|\lambda_1\rangle$ matches $|l_1\rangle$ and so on). There is left a set of unmatched exact states $\{|\mu\rangle\}$ and unmatched tensor network states $\{|m\rangle\}$.

We can now use the pairing structure on approximate eigenstates to inform new matches. An unmatched approximate eigenstate $|m\rangle$ has a set of j partners in $\{|l_k\rangle\}$ which each have matches in $\{|\lambda_m\rangle\}$. Conveniently, the approximate τ_i^x operators produced from the tensor network algorithm give us the transformations from $|m\rangle$ to its j partners in the already matched set $\{|l_{j,m}\rangle\}$. If the same transformations roughly take the exact eigenstate matches of $\{|l_{j,m}\rangle\}$, labeled $\{|\lambda_{j,m}\rangle\}$, to an unmatched exact eigenstate $|\mu\rangle$, then we match $|\mu\rangle$ and $|m\rangle$. To make assignments iteratively, we find these new matches one at a time by scanning over $\{|\mu\rangle\}$ and $\{|m\rangle\}$ to find the eigenstates from each eigenstate that maximally fit this pattern. Once a match is made, it can be used to inform new matches in new iterations. Figure 1 illustrates this relation.

To this end, we find the eigenstates in $\{|\mu\rangle\}$ and $\{|m\rangle\}$ that maximize the function

$$f(\mu, m) = \sum_{i\in s(m)} |\langle\lambda_{i,m}|\tau_i^{x,\mathrm{TN}}|\mu\rangle|^2, \tag{5}$$

where $\tau_i^{x,\mathrm{TN}}$ is the l-bit operator yielded from the tensor network approximation, $s(m)$ is the set of sites j where the j partner of $|m\rangle$ is in $\{|l_k\rangle\}$, and $|\lambda_{i,m}\rangle$ is the exact eigenstate matched to the i partner of $|m\rangle$.

After finding the maximizing values of $|\mu\rangle$ and $|m\rangle$ for Eq. (5), we match these two states, add them to the set of matched states, and iterate until all matches have been made. At larger system sizes and for lower disorder strengths, the number of unmatched states can make this process computationally expensive. As such, making more than one assignment on each iteration expedites the process.

After a complete set of pairings is made, operators are constructed as described in Eqs. (2)–(4).

The phase of the eigenstates produced by exact diagonalization presents another consideration. The eigenstates produced by exact diagonalization are allowed an arbitrary scalar phase. Because our Hamiltonian is real and can therefore be diagonalized by an orthogonal matrix, MATLAB produces eigenstates with arbitrary sign. However, the sign of the eigenstates affects the calculation of τ_i^x and τ_i^y as shown in Eqs. (2) and (3), requiring us to choose the "correct" sign in order to construct l-bit operators. Note that the calculation of τ_i^z as shown in Eq. (4) is unaffected by the sign.

To choose the sign of an eigenstate after the matching process is completed, we use the following algorithm: For an eigenstate and its i partner $|\alpha\rangle$ and $|\beta_{i,\alpha}\rangle$, we take $\hat{O} = \mathrm{Tr}_{\bar{i}}[|\alpha\rangle\langle\beta_{i,\alpha}| + |\beta_{i,\alpha}\rangle\langle\alpha|]$, where $\mathrm{Tr}_{\bar{i}}$ is a partial trace over all sites except for i. If $\hat{O}$ resembles σ_x, the signs of both eigenstates remain unchanged. If $\hat{O}$ resembles $-\sigma_x$, then the sign of $|\beta_{i,\alpha}\rangle$ is flipped. The sign of $|\beta_{i,\alpha}\rangle$ is then set and the process is repeated until all eigenstates have been assigned a sign. After this process is completed $\hat{O}$ should resemble σ_x for any pair $|\alpha\rangle$ and $|\beta_{i,\alpha}\rangle$. However the assignment of sign could not be carried out generically for all pairs. Although this does not change the algebraic properties of the operators, it does effect their localization lengths.

In order to characterize the localization properties of our exact l-bit operators, we propose a measure of localization length of an operator. Any operator $\hat{O}$ can generally be written in the form $\hat{O} = \sum_{\gamma\in\{0,x,y,z\}} A_i^\gamma \otimes \sigma_i^\gamma$, for any site i. Here σ^0 is the identity operator and the matrices A_i^γ act on all sites that are not i.

An operator is local to a site i if for $j \neq i$, $A_j^x = A_j^y = A_j^z = \mathbb{0}$. Thus, a scalar value for the weight of an operator at site i is given by $\mathrm{Tr}[A_i^{x\,2} + A_i^{y\,2} + A_i^{z\,2}]$. For a maximally local operator located on site i, $w_j = 0$ for all $j \neq i$. We define

$$w_i(\hat{O}) \equiv 8 \sum_{\gamma\in\{x,y,z\}} \mathrm{Tr}\big(A_i^{\gamma\,2}\big) = \sum_\gamma \mathrm{Tr}\big[\big(\hat{O} - \sigma_i^\gamma \hat{O}\sigma_i^\gamma\big)^2\big]. \tag{6}$$

For a quasilocal operator, the weight of an operator centered on site i should decay as $e^{-|i-j|/\xi_z}$. In fact, Fig. 2

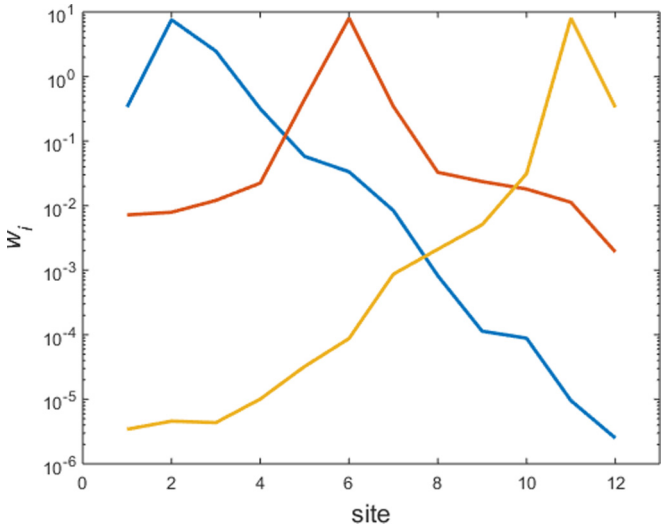

FIG. 2. Weight functions $w_i(\tau_z)$ [see Eq. (6)] showing exponential decay with position for three τ_z operators. Operators shown are for a single disorder realization at $h = 8$.

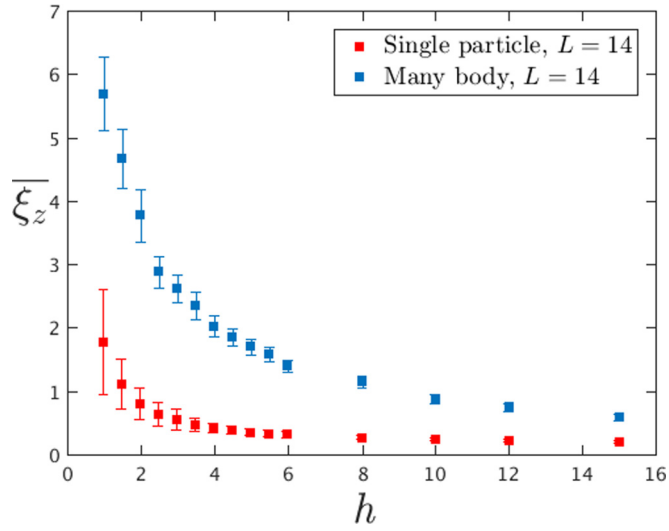

FIG. 3. Plot of mean localization length ($\overline{\xi}_z$) of τ_i^z operators and mean localization length of single-particle Anderson localized eigenstates, both for system sizes $L = 14$. Error bars indicate the standard deviation of the distribution of localization lengths.

shows the exponential decay of three τ^z operators for a single disorder realization at $h = 8$ for system size $L = 12$.

A best fit curve is calculated on the weight function of the operator from the peak weight to the furthest edge. The process is explicitly carried out by taking a linear fit on the natural logarithm of the weight at each site minus the weight at the boundary.

Exponential decays are robust for a wide range of disorder strengths. Deep in the localized phase at $h = 10$ for $L = 14$, the linear fits have an average $R^2 = 0.85$. Moving into the thermal phase, the average R^2 remains relatively high, indicating that some operators retain exponential decay characteristics. At $h = 6$, the average $R^2 = 0.84$. At $h = 4$, the average $R^2 = 0.86$. At $h = 1$, the average $R^2 = 0.80$.

This algorithm finds highly localized operators that commute with the Hamiltonian and with one another, but not necessarily the most local ones.

l-bit operator localization lengths can be expected to behave qualitatively as single-particle eigenstate Anderson localization lengths, whose behavior has been extensively studied. In spin language, the noninteracting, disordered fermion hopping Hamiltonian is

$$H = \sum_{i=1}^{L-1} \left(S_i^x S_{i+1}^x + S_i^y S_{i+1}^y \right) + \sum_{i=1}^{L} h_i S_i^z, \tag{7}$$

where the values h_i are once again independently drawn from a uniform distribution $[-W, W]$.

A comparison between l-bit localization lengths constructed on MBL systems and single particle localization lengths is shown in Fig. 3. In general, the localization lengths for single-particle systems are lower, though both obey a power-law relationship with disorder. The mean single particle localization length roughly follows the form $\overline{\xi} \propto (h - h_{\text{offset}})^{-0.57}$, where h_{offset} is some adjustment to the disorder strength due to finite-size effects; Anderson localization is known to exist for infinitesimal disorder in one dimension. The form of the MBL localization length relationship with disorder strength h is discussed further in the next section.

IV. DISTRIBUTION OF LOCALIZATION LENGTHS AND MBL TRANSITION

A. Mean localization lengths

A rigorous proof of the existence of l-bit operators for MBL is valid only deep in the localized phase [12,13]. A systematic construction procedure of exact l-bits provides a tool to study their statistical properties close to the MBL transition For instance, how do the statistics of the localization length of the operators vary in vicinity of the transition? Deep in the MBL phase, the exponential rarity of l-bits with large localization lengths is crucial for their stability to perturbations on the Hamiltonian. On approaching the transition, the increased likelihood of l-bits with large localization lengths may render these operators unstable raising the possibility of alternative effective description of localization near the transition [17]. The method developed here allows us to probe the properties of the length scale of l-bit operators which are always exactly conserved by construction.

Using approximately 130 realizations for each disorder strength at four different system sizes ($L = 8, 10, 12, 14$), we find a systematic increase in the average localization length of the τ_i^z operators with decreasing h. Deep in the localized phase ($h \sim 8$) the localization length is of the order of, or even less than, a single lattice spacing. For systems of size $L = 14$, at $h = 5$ the average localization length $\overline{\xi}_z = 1.71$ and well into the MBL phase $\overline{\xi}_z = 0.60$ at $h = 15$. As the Hamiltonian approaches the transition into the thermal phase at lower disorder strengths, the average localization length of the τ_i^z operator increases for all system sizes, as indicated in Fig. 4.

We conducted a scaling collapse for the function $\overline{\xi}_z/\overline{\xi}_z(h_{\text{crit}}) = F[L^{1/\nu}(h - h_{\text{crit}})]$, shown in Fig. 4. Optimal values for the fit are found at $h_{\text{crit}} = 3.5$ and $1/\nu = 0.9$

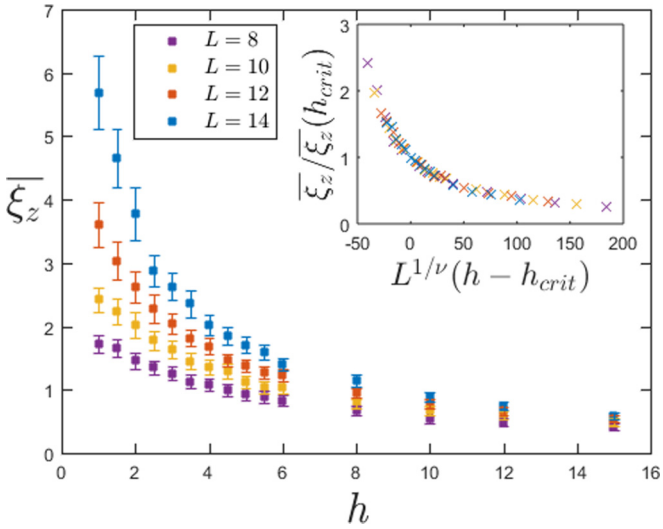

FIG. 4. Plot of mean localization length ($\overline{\xi}_z$) of τ_i^z operators for different system sizes (L) and disorders (h). Error bars indicate the standard deviation of the distribution of localization lengths for each length and disorder. In the inset, a scaling collapse with $\nu = 1.1$ and $h_{\text{crit}} = 3.5$ is presented. Those values were obtained by optimizing a polynomial fit on $\overline{\xi}_z/\overline{\xi}_z(h_{\text{crit}})$.

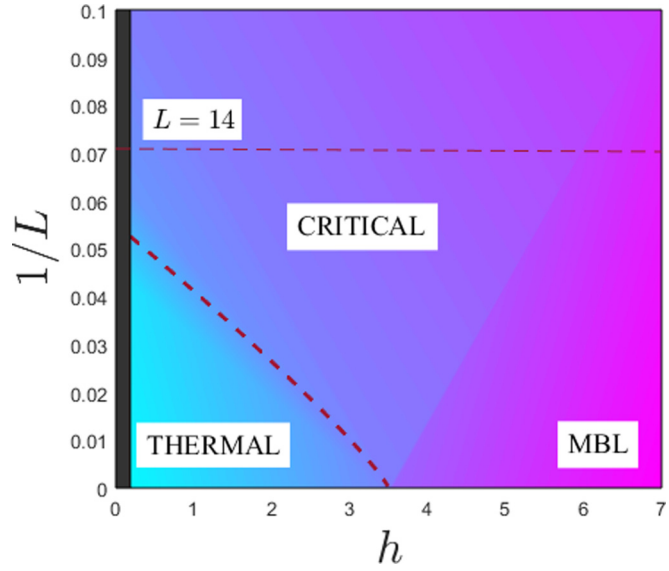

FIG. 5. A schematic diagram showing the phases of the random field Heisenberg spin chain and the quantum critical crossover regime as a function of disorder h and inverse system size L. The bold dashed line represents the crossover scale (h_{cross}) between the thermal and the quantum critical regime. The region where h is close to zero is purposely obscured; at low disorder, integrability effects are likely to be relevant. For the system sizes we have access to, the average localization still remains much smaller than L which is an indication that we are in the quantum critical regime.

according to a least-square fit. Furthermore, the function F is shown to be of the form $F(x) \propto (x + x_\infty)^{-\alpha}$, where $x_\infty = 48$ and $\alpha = 0.55$. The scaling collapse of the mean and typical localization lengths are similar without significant variation in parameters. The correlation length exponent ν is smaller than the finite-size scaling bounds on ν provided by the Harris criterion for the MBL transition [33], much like other exact diagonalization studies. The scaling function gives an insight into the thermal to quantum critical crossover regime. The fact that there are l-bits with localization length $\xi_z \ll L$ around the critical disorder strength suggests that the system is in the crossover regime for these system sizes. The form of the scaling function $F(x)$ provides a relationship between system size and crossover disorder strength $h_{\text{cross}}(L)$, which describes the regime at which the l-bit localization length diverges. This is shown in the schematic phase diagram Fig. 5 which is consistent with the picture of the transition given in [16]. The scaling collapse gives an estimate of this crossover scale on the thermal side of the transition,

$$h_{\text{cross}}(L) = 3.5 - \frac{48}{L^{0.9}}. \tag{8}$$

The crossover between the critical and MBL regimes, which is expected in equilibrium second order transition, is not visible in this quantity. A study of the l-bits with large localization lengths near the transition can contain information of the resonant cluster responsible for the entire crossover regime as seen in phenomenological renormalization group studies [14,15].

B. Distribution of localization lengths

The full distribution of localization lengths $P(\xi_z)$ sheds further light on the fate of the exact l-bits. The histograms of the localization lengths for two representative disorder strengths at system size $L = 14$ are shown in Fig. 6. The distribution of localization lengths changes qualitatively with disorder strength. As shown in Fig. 6(b), at $h = 10$ the peak of the distribution is below $\xi_z = 1$ with the majority of operators being localized within a single lattice spacing. The tails of the distribution show that operators with larger localization lengths are exponentially rare, $P(\xi_z) \sim \exp(-\xi_z/\Theta)$. Hence, these operators are stable to local perturbations in the Hamiltonian. The fitted value is $\Theta = 0.32$ for $h = 10$.

On reducing the disorder strength to $h = 4$, the peak of the distribution shifts to $\xi_z > 1$. As the system approaches the critical point, a large fraction of operators have $\xi_z > 1$ and the tail of the distribution can be fitted to an exponential decay $P(\xi_z) \sim \exp(-\xi_z/\Theta)$ or a power law $P(\xi_z) \sim \xi_z^{-\eta}$ equally well, as shown in Fig. 6(a). Although there continue to exist operators with $\xi_z \approx 1$, a large part of the weight of the distribution moves to larger ξ_z. This shows that the l-bit operators with large localization length are more probable close to the transition in comparison to the l-bits at large disorder. Interestingly, on reducing the disorder below the critical disorder strength h_{crit}, we find operators with $\xi_z \approx 1$ for our finite size systems. Although they form a small fraction of the distribution, it suggests that even in the "thermal" phase close to the transition there are local operators which commute exactly with the Hamiltonian. The presence of such operators is in striking contrast to the traditional understanding of non-integrable models. (Although there are now studies of edge mode operators with very long lifetimes even in models with broken integrability [34].) It will be interesting to study the

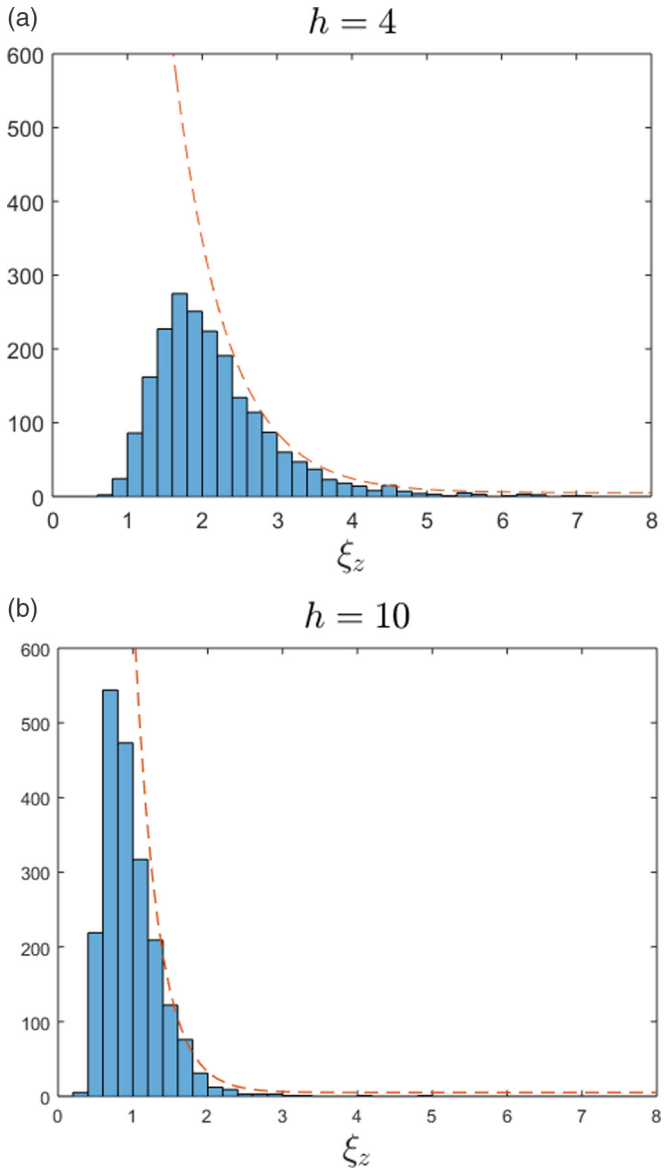

FIG. 6. Histograms of localization lengths of τ_i^z at system size $L = 14$. The decay of the tail of each histogram is shown as a dashed line. An exponential decay fit, $P(\xi_z) \propto e^{-\xi_z/\Theta}$ was performed on each graph from the peak of the distribution to the edge. Weaker disorder systems, here $h = 4$, fit to exponential decay models with decay coefficient $\Theta = 0.70$ and error $R^2 = 0.98$ and to a power law $[P(\xi_z) \propto \xi_z^{-\eta}]$ with decay coefficient $\eta = 6.5$ and error $R^2 = 0.97$, equally well. Stronger disorder systems, here $h = 10$, fit most strongly to exponential decay models with decay coefficient $\Theta = 0.32$ and error $R^2 = 0.98$.

role of these operators in the slow dynamics observed in the thermal regime close to the transition [35].

V. CONCLUSION

In this article we presented a technique to construct the exact l-bit operators comprising the quasilocal τ_i^z operators which commute with the Hamiltonian. We did so by implementing the pairing structure on approximate eigenstates produced using the tensor network method from [28]. We constructed l-bit operators by matching the approximate eigenstates to the exact eigenstates. We found that the l-bit operators exhibit weight functions w_i [see Eq. (6)] that decay exponentially away from their localization centers.

Mean localization length of τ_i^z operators increases from less than a lattice spacing at large disorder to a fraction of the system size close to the transition. This increase is consistent with a power-law divergence at $h \approx 3.5$ which is close to other exact diagonalization studies. A scaling collapse of the average localization length using a power law yields an exponent $\alpha \approx 0.55$ and correlation length exponent $\nu = 1.1$. We find further that the distribution of localization length ξ_z changes qualitatively as a function of disorder strength. At disorder strength close to the phase transition, the distribution of localization lengths shows a peak with tails which can be fitted to a power law, where the exponent of the power changes continuously with disorder (exponential fits are also reasonable). At higher disorder strengths, the peak of the distribution shifts to lower values with exponentially decaying tails.

Our results have several important implications for the MBL transition into the thermal phase. The power-law distribution of the length scales is consistent with the strong-disorder renormalization group studies of the MBL transition in coarse-grained phenomenological models [14,15]. For finite-size systems, our treatment provides the crossover scale between thermal and the quantum critical regimes for a microscopic model [16]. The spatial structure of the operators with large localization lengths can be used to detect the backbone resonant structure which is expected to lead to thermalization. If the power-law distribution of localization lengths was to survive in the thermodynamic limit, it would suggest an intermediate phase with coexisting localized and delocalized operators. It would be interesting to search for an effective description of such a phase and its relationship to l*-bit phenomenology [17]. An interesting observation is the existence of local operators below the critical disorder strength of $h_{\text{crit}} \approx 3.5$, such as $h = 3$. This suggests that the quantum critical regime may be dominated by fluctuations which appear localized.

Note added. Recently, we became aware of the independent similar work presented in Refs. [36,37].

ACKNOWLEDGMENTS

We would like to thank Fabian Essler and Paul Fendley for helpful discussions. S.H.S. and T.B.W. are both supported by TOPNES, EPSRC Grant No. EP/I031014/1. S.H.S. is also supported by EPSRC Grant EP/N01930X/1. The work of A.P. was performed in part at the Aspen Center for Physics, which is supported by National Science Foundation Grant PHY-1066293. T.B.W. would like to thank the European Commission for support under the Marie Curie Programme. The contents of this article reflect only the authors views and not the views of the European Commission.

Statement of compliance with EPSRC policy framework on research data: This publication is theoretical work that does not require supporting research data.

[1] A. Polkovnikov, K. Sengupta, A. Silva, and M. Vengalattore, Nonequilibrium dynamics of closed interacting quantum systems, Rev. Mod. Phys. **83**, 863 (2011).

[2] D. M. Basko, I. L. Aleiner, and B. L. Altshuler, Metal–insulator transition in a weakly interacting many-electron system with localized single-particle states, Ann. Phys. **321**, 1126 (2006).

[3] I. V. Gornyi, A. D. Mirlin, and D. G. Polyakov, Interacting Electrons in Disordered Wires: Anderson Localization and Low-*t* Transport, Phys. Rev. Lett. **95**, 206603 (2005).

[4] A. Pal and D. A. Huse, Many-body localization phase transition, Phys. Rev. B **82**, 174411 (2010).

[5] V. Oganesyan and D. A. Huse, Localization of interacting fermions at high temperature, Phys. Rev. B **75**, 155111 (2007).

[6] R. Nandkishore and D. A. Huse, Many-body localization and thermalization in quantum statistical mechanics, Annu. Rev. Condens. Matter Phys. **6**, 15 (2015).

[7] M. Schreiber, S. S. Hodgman, P. Bordia, H. P. Lüschen, M. H. Fischer, R. Vosk, E. Altman, U. Schneider, and I. Bloch, Observation of many-body localization of interacting fermions in a quasirandom optical lattice, Science **349**, 842 (2015).

[8] J. Smith, A. Lee, P. Richerme, B. Neyenhuis, P. W. Hess, P. Hauke, M. Heyl, D. A. Huse, and C. Monroe, Many-body localization in a quantum simulator with programmable random disorder, Nat. Phys. **12**, 907 (2016).

[9] D. A. Huse, R. Nandkishore, V. Oganesyan, A. Pal, and S. L. Sondhi, Localization-protected quantum order, Phys. Rev. B **88**, 014206 (2013).

[10] A. Chandran, V. Khemani, C. R. Laumann, and S. L. Sondhi, Many-body localization and symmetry-protected topological order, Phys. Rev. B **89**, 144201 (2014).

[11] Y. Bahri, R. Vosk, E. Altman, and A. Vishwanath, Localization and topology protected quantum coherence at the edge of hot matter, Nat. Commun. **6**, 7341 (2015).

[12] J. Z. Imbrie, On many-body localization for quantum spin chains, J. Stat. Phys. **163**, 998 (2016).

[13] J. Z. Imbrie, Diagonalization and Many-Body Localization for A Disordered Quantum Spin Chain, Phys. Rev. Lett. **117**, 027201 (2016).

[14] R. Vosk, D. A. Huse, and E. Altman, Theory of the Many-Body Localization Transition in One-Dimensional Systems, Phys. Rev. X **5**, 031032 (2015).

[15] A. C. Potter, R. Vasseur, and S. A. Parameswaran, Universal Properties of Many-Body Delocalization Transitions, Phys. Rev. X **5**, 031033 (2015).

[16] V. Khemani, S. P. Lim, D. N. Sheng, and D. A. Huse, Critical Properties of the Many-Body Localization Transition, Phys. Rev. X **7**, 021013 (2017).

[17] A. Chandran, A. Pal, C. R. Laumann, and A. Scardicchio, Many-body localization beyond eigenstates in all dimensions, Phys. Rev. B **94**, 144203 (2016).

[18] W. De Roeck and F. Huveneers, Stability and instability towards delocalization in many-body localization systems, Phys. Rev. B **95**, 155129 (2017).

[19] T. Wahl, A. Pal, and S. H. Simon, Signatures of the many-body localized regime in two dimensions, arXiv:1711.02678.

[20] For the purposes of this work, we'll always consider FMBL systems and for the sake of brevity use the term MBL. Although it is important to keep in mind that the phenomena of MBL can be more general.

[21] D. A. Huse, R. Nandkishore, and V. Oganesyan, Phenomenology of fully many-body-localized systems, Phys. Rev. B **90**, 174202 (2014).

[22] M. Serbyn, Z. Papić, and D. A. Abanin, Local Conservation Laws and the Structure of the Many-Body Localized States, Phys. Rev. Lett. **111**, 127201 (2013).

[23] V. Ros, M. Mueller, and A. Scardicchio, Integrals of motion in the many-body localized phase, Nucl. Phys. B **891**, 420 (2015).

[24] D. Pekker, B. K. Clark, V. Oganesyan, and G. Refael, Fixed Points of Wegner-Wilson Flows and Many-Body Localization, Phys. Rev. Lett. **119**, 075701 (2017).

[25] L. Rademaker and M. Ortuño, Explicit Local Integrals of Motion for the Many-Body Localized State, Phys. Rev. Lett. **116**, 010404 (2016).

[26] L. Rademaker, M. Ortuño, and A. M. Somoza, Many-body localization from the perspective of integrals of motion, Ann. Phys. **529**, 1600322 (2017).

[27] A. Chandran, I. H. Kim, G. Vidal, and D. A Abanin, Constructing local integrals of motion in the many-body localized phase, Phys. Rev. B **91**, 085425 (2015).

[28] T. B. Wahl, A. Pal, and S. H. Simon, Efficient Representation of Fully Many-Body Localized Systems Using Tensor Networks, Phys. Rev. X **7**, 021018 (2017).

[29] F. Pollmann, V. Khemani, J. I. Cirac, and S. L. Sondhi, Efficient variational diagonalization of fully many-body localized Hamiltonians, Phys. Rev. B **94**, 041116(R) (2016).

[30] D. Pekker and B. K. Clark, Encoding the structure of many-body localization with matrix product operators, Phys. Rev. B **95**, 035116 (2017).

[31] A. Chandran, J. Carrasquilla, I. H. Kim, D. A. Abanin, and G. Vidal, Spectral tensor networks for many-body localization, Phys. Rev. B **92**, 024201 (2015).

[32] D. J. Luitz, N. Laflorencie, and F. Alet, Many-body localization edge in the random-field Heisenberg chain, Phys. Rev. B **91**, 081103 (2015).

[33] A. Chandran, C. R. Laumann, and V. Oganesyan, Finite size scaling bounds on many-body localized phase transitions, arXiv:1509.04285.

[34] J. Kemp, N. Y. Yao, C. R. Laumann, and P. Fendley, Long coherence times for edge spins, J. Stat. Mech.: Theory Exp. **2017**, 063105 (2017).

[35] K. Agarwal, S. Gopalakrishnan, M. Knap, M. Müller, and E. Demler, Anomalous Diffusion and Griffiths Effects Near the Many-Body Localization Transition, Phys. Rev. Lett. **114**, 160401 (2015).

[36] M. Goihl, M. Gluza, C. Krumnow, and J. Eisert, Construction of exact constants of motion and effective models for many-body localized systems, Phys. Rev. B **97**, 134202 (2018).

[37] S. J. Thomson and M. Schiró, Time evolution of many-body localized systems with the flow equation approach, Phys. Rev. B **97**, 060201 (2018).